Rapid Communications

Front propagation into an unstable state in a forced medium: Experiments and theory

K. Alfaro-Bittner,[1] C. Castillo-Pinto,[2] M. G. Clerc,[2] G. González-Cortés,[2] R. G. Rojas,[1] and M. Wilson[3]
[1]*Instituto de Física, Pontificia Universidad Católica de Valparaíso, Casilla 4059, Valparaíso, Chile*
[2]*Physics Department and Millennium Institute for Research in Optics, Facultad de Ciencias Físicas y Matemáticas, Universidad de Chile, Casilla 487-3, Santiago, Chile*
[3]*CONACYT-CICESE, Carretera Ensenada-Tijuana 3918, Zona Playitas, CP 22860, Ensenada, Mexico*

(Received 13 August 2018; published 7 November 2018)

Spatially forced systems can exhibit coexistence and a rich interface dynamics between manipulable states. We show here how the propagation speed of a front into an unstable state can be modified through periodic space forcing. Based on optical feedback, we set up a quasi-one-dimensional forced experiment in a liquid-crystal cell. When changing the forcing parameters, fronts exhibit a ratchet motion. Unexpectedly, the average speed of fronts decreases when the strength of the forcing increases. Close to molecular reorientation transition, an amplitude equation allows characterizing analytically and numerically the observed dynamics.

DOI: 10.1103/PhysRevE.98.050201

Introduction. Macroscopic systems with injection and dissipation of energy are characterized by exhibiting stable attractive equilibria [1,2]. The features of these equilibria are characterized by the physical parameters of the system under study. Those parameters, that can be manipulated externally, are called control parameters. When one of the control parameters surpasses a critical value, the equilibrium loses stability giving rise to new equilibria or transiting to a different equilibrium. This phenomenon corresponds to a bifurcation [1–4], since, it corresponds to a qualitative change of the dynamics of the system under study [3]. The bifurcations mentioned above correspond to a supercritical and subcritical transition, respectively. A hysteresis loop characterizes subcritical transitions. Indeed, the system exhibits coexistence of equilibria. In this region of parameters, due to the inherent fluctuations of macroscopic systems and physical imperfections, one observes domains between the different states of equilibrium [4], which are separated by domain walls. Due to the relative stability properties between these equilibria, the interfaces between domains are propagative, generating a complex spatiotemporal dynamics. These interfaces are known as front interfaces, domain walls, or wave fronts depending on the physical context where they are observed [4–19]. These solutions correspond to nonlinear waves. Front dynamics has been observed in diverse contexts, such as walls separating magnetic domains, liquid-crystal phases, fluidized granular states, chemical reactions, solidification and combustion processes, and populations dynamics, to mention a few. Indeed, interface dynamics is a robust phenomenon ranging from chemistry and biology to physics. The propagation and dynamics of fronts depend on the nature of the states that are being connected. The invasion of the stable state into the unstable one usually characterizes fronts between stable and unstable state. The studies of combustion propagation of Faraday [8], gene propagation of Fisher [9], and Kolmogorov *et al.* [10] are pioneering studies in the understanding of this phenomenon. In honor of these baseline studies, the fronts into unstable state are usually called *FKPP fronts* (see [12], and references therein). The propagation speed and shape of these fronts depend on the initial conditions. In the case of bounded initial conditions, the front always propagates asymptotically with the minimum speed [13]. FKPP fronts have been observed in Taylor-Couette instability [14], Rayleigh-Bénard convection [15], pearling and pinching on the propagating Rayleigh instability [16], spinodal decomposition in polymer mixtures [17], liquid-crystal light valves with optical feedback [18], and population dynamics [5]. In all these observations, the dynamics between states of spontaneous equilibrium are analyzed. The mastering and manipulation of these fronts propagations will allow controlling the impact of these nonlinear waves in several contexts, in particular, in the combustion process, crystal growth, and spread of infectious diseases.

A simple strategy that can handle the nonlinear wave propagation using the spatial forcing is presented. This Rapid Communication aims to study the propagation of fronts into an unstable state in a spatially forced medium. We investigate front propagation into an unstable state in a one-dimensional configuration. Based on optical feedback with a spatially amplitude modulated beam, we set up a quasi-one-dimensional forced experiment in a nematic liquid-crystal cell. The molecular reorientation as a function of the applied voltage in a liquid-crystal light valve exhibits a subcritical Fréedericksz transition [18]. By changing the forcing parameters, the front into unstable state exhibits an oscillatory ratchet motion. The average speed of fronts decreases when the forcing strength increases. Theoretically, close to the Fréedericksz transition, we consider an amplitude equation that accounts for the observed subcritical bifurcation and spatial forcing. In the limit of weak forcing, we can derive an analytical expression for the front speed, which has a quite fair agreement with the numerical simulations. In addition, we have numerically characterized the front speed with respect to the forcing parameters.

Experimental description. Liquid-crystal light valve (LCLV) with an optical feedback loop is an optical experiment that exhibits a transition of molecular reorientation of

 ©2018 American Physical Society

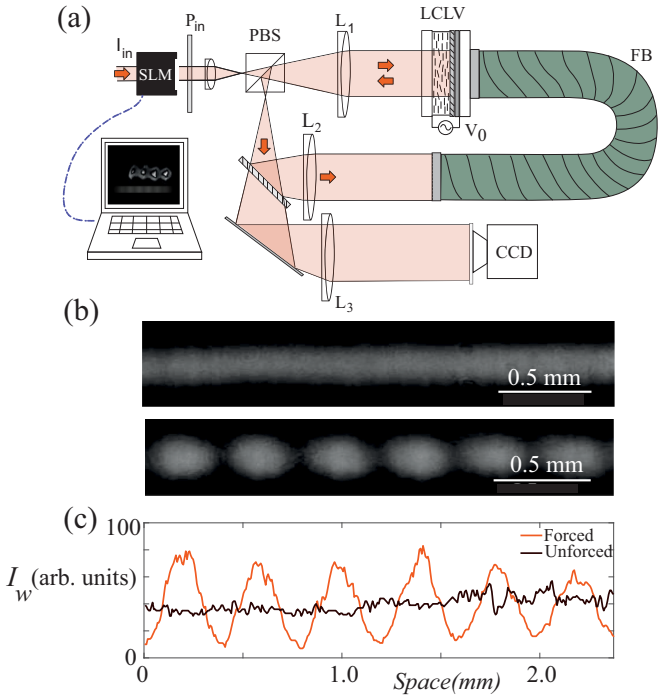

FIG. 1. Liquid-crystal light valve (LCLV) setup. (a) Schematic representation of the liquid-crystal light valve with optical feedback. I_{in} is the input light intensity, P_{in} is a polarizer, PBS is the polarized beam splitter, L_1, L_2, and L_3 are lenses, V_0 is the external voltage applied, FB is the fiber bundle, and CCD is the camera that captures the images. (b) Snapshots of the LCLV without optical feedback with the unforced and the forced masks applied. (c) Intensity profiles of the liquid-crystal cell with and without forcing in (b).

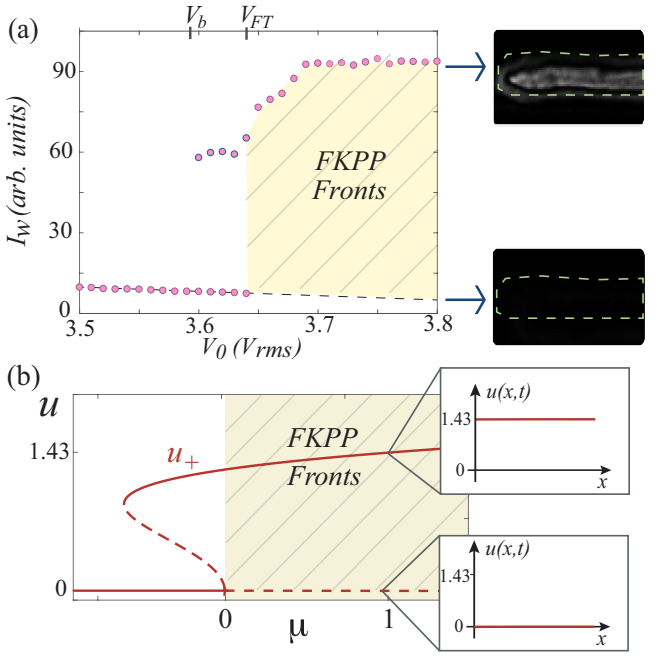

FIG. 2. (a) Experimental bifurcation diagram performed in a liquid-crystal light valve with optical feedback, intensity I_w as a function of the applied voltage V_0. The points correspond to values of total light intensity I_w at the LCLV. The dashed line is a schematic representation of the aligned molecular state induced by the anchoring of the walls. The painted area accounts for the region of coexistence between stable and unstable state, where FKPP fronts are observed. The insets are the snapshot of the typically observed states. (b) Bifurcation diagram of model Eq. (1) without spatial forcing ($\gamma = 0$) as a function of bifurcation parameter μ with $\beta = 0.8$. Continuous and dashed lines account for stable and unstable state, respectively. The painted area accounts for the region of coexistence between stable and unstable state. The insets stand for typically observed states.

subcritical type [20]. The experimental setup is schematically represented in Fig. 1. The LCLV is composed of a thin nematic liquid-crystal film between a glass and a photoconductive plate over which a dielectric mirror is deposed. The liquid-crystal film has planar alignment with thickness $d = 15$ [μm]. The liquid crystal used is a nematic LC-654 (NIOPIK). It is a mixture of cyanobiphenyls, with a positive dielectric anisotropy $\varepsilon_a = 10.7$ and large optical birefringence $\Delta n = 0.2$. The photoconductor behaves like a variable resistance, which decreases for increasing illumination. Liquid-crystal light valve with optical feedback has been studied extensively in the literature (see review article [21], and references therein).

Transparent electrodes over the glass plates allow the application of voltage V_0 inducing an electric field. The LCLV is illuminated by an He-Ne laser beam ($\lambda = 632.8$ [nm]) with intensity $I_{\text{in}} = 35$ [mW]. The laser beam passes through a Holoeye LC 2002 transmissive spatial light modulator (SLM), allowing us to manipulate the spatial profile of the intensity controlling therefore the front dynamics and imposing a quasi-one-dimensional configuration $I_{\text{in}}(x) = I_{\text{in}} + I_k \cos(kx)$. The optical path is schematically represented in Fig. 1(a). Over a critical voltage, i.e., Fréedericksz voltage V_{FT}, the molecules tend to align along the direction of the applied electric field. The molecular orientation changes locally and dynamically following the spatial illumination distribution present in the photoconductor wall of the cell. The light-driven feedback is obtained by sending back onto the photoconductor, I_w, the light which has passed through the liquid-crystal layer and has been reflected by the dielectric mirror. The light beam experiences a phase shift which depends on the liquid-crystal orientation (see [21], and references therein). By inserting a polarized beam splitter, phase shifts are converted into intensity variations modulating the illumination onto the photoconductor, and hence the effective voltage applied to the liquid-crystal layer. Finally, the laser beam is directed to a charge-coupled device (CCD) camera where the images of the LCLV are taken.

Experimental results. Using the SLM, we have illuminated a channel in the LCLV of 3.5 mm long and 0.25 mm wide (see the rectangles of the upper panels of Fig. 3). Indeed, the nature of the system is almost one dimensional. For low external voltages, no change is observed. The illuminated area remains dark, which is a manifestation of no molecular reorientation [see bottom inset in Fig. 2(a)]. Above a critical value V_{FT}, the region begins to change color to gray [see top panels in Figs. 1(b) and 2]. The experimental bifurcation diagram of this transition is illustrated in Fig. 2(a). The intensity change of the illuminated area is abrupt, which is consistent

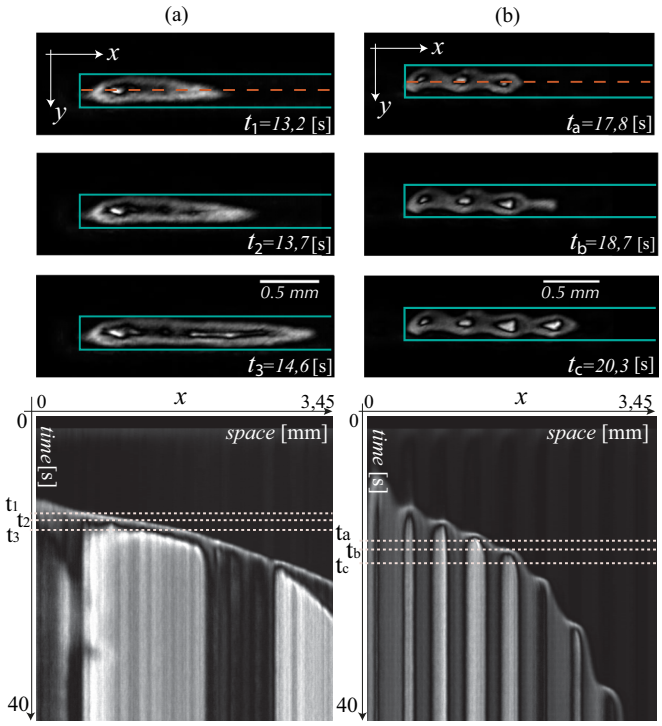

FIG. 3. Experimental front propagation, snapshots, and respective spatiotemporal diagrams of (a) an unforced medium and (b) a forced one observed at $V_0 = 3.69$ (V_{rms}). The upper panels account for a temporal sequence of snapshots. The rectangle accounts for the illuminated area with optical feedback, and the dashed curve is the extracted region to obtain the spatiotemporal diagrams. The bottom panels stand for the spatiotemporal evolution of the fronts in the unforced and the forced system, respectively. The horizontal dashed lines account for the moments where the top snapshots are extracted.

with a subcritical molecular reorientation transition [20]. Characterization of this instability using the total intensity is consistent with the subcritical Fréedericksz transition [see Fig. 2(a)]. Namely, increasing the voltage ($V > V_{\text{FT}}$), the gray state changes slightly. Similarly, decreasing the voltage, the gray state is maintained until a critical value $V_b < V_{\text{FT}}$. Hence, the system exhibits a hysteresis or bistable region. Note that the Fréedericksz transition from black to gray region is characterized by the emergence of a gray spot that begins invading the system. This phenomenon corresponds to a FKPP front propagation between the unstable (black region) to the stable state (gray region). Figure 3(a) shows this phenomenon observed at $V_0 = 3.69$ (V_{rms}). Note that as a consequence of the inevitable imperfections of the experiment [see Fig. 1(c)], as the front propagates, the speed slightly changes. The average speed of propagation is 3.3 (mm/s). In most of the observed cases, the fronts are triggered from the edges of the illuminated region (see top panels of Fig. 3). The previous scenario changes if we consider a spatial modulation of the applied light. We observe that the gray state becomes a spatially modulated state. Figures 1(b) and 1(c) show, respectively, the state and its profile before and after applying a modulation to the illumination light to the LCLV. The modulated state can be understood as a spatial modulated light inducing a voltage on the spatially modulated liquid crystal orientation. Likewise, note that although the light is modulated, the non-reoriented (black) state is not modulated since the light induces a parametric effect on the dynamics of molecular reorientation [20]. Hence, in the forced case one expects to observe fronts between a stable induced periodic state and an unstable uniform one. Figure 3 shows a front propagation between these states. Unexpectedly, the front speed into unstable state in a forced medium is slower. Note that the speed is at least three times smaller. Therefore, by means of spatially modulated forcing, one can control the propagation speed of the front.

Theoretical description. Based on the elastic theory with the inclusion of electrical terms that account for the optical feedback and the applied voltage, close to the Fréedericksz transition, the liquid-crystal molecules begin to reorient. The molecular orientation is characterized by the director $\vec{n} \approx [u\ \sin(k\pi/d), 0, 1 - u^2 \sin^2(k\pi/d)]$ [20], where $u(x,t)$ accounts for the most unstable spatial mode. This mode satisfies the following dimensionless equation [20]:

$$\partial_t u = [\mu + \gamma \sin(kx)]u + \beta u^2 + u^3 - u^5 + \partial_{xx} u, \qquad (1)$$

where x and t, respectively, account for the spatial transverse coordinate and time, μ is the bifurcation parameter that accounts for the competition between the electric and elastic force, and $\mu = 0$ corresponds to the reorientation transition point. γ and k stand for to the amplitude and the wave number of the forcing, respectively. Namely, γ is proportional to input light intensity I_{in}. β is a phenomenological parameter that accounts for the pretilt induced by the anchoring in the walls of the liquid-crystal layer. The methodology of how to derive the parameters $\{\mu, \alpha, \beta\}$ and the relation with the physical parameters are given in Ref. [20]. The γ parameter, using the same procedure, has the form $\gamma \equiv \alpha\epsilon_a I_k[\epsilon_a \cos(kd\Delta n)(dI_{\text{in}}\alpha[1 + \cos(2kd\Delta n)] + 2V_0) + \epsilon_0 kd\Delta n \cos(kd\Delta n)(dI_{\text{in}}\alpha[1 + \cos(kd\Delta n)] + V_0)]/d$. The term proportional to β breaks the reflection symmetry of amplitude u. This effect always renders the transition into a discontinuous with a small hysteresis. Nonlinearities in model Eq. (1) stand for the competition between elastic and electrical forces induced by optical feedback [20]. The last term of Eq. (1) describes the transverse elastic coupling. Note that the amplitude $u(x,t)$ has no physical sense when it is negative. The theoretical model is valid near the reorientational transition when the system exhibits a small hysteresis cycle. However, in that region, experimentally it is difficult to control the spatial forcing, since the light intensity is weak ($I_{\text{in}} \ll 1$). Therefore, the theoretical model Eq. (1) qualitatively describes the experiment.

Figure 2(b) illustrates the typical bifurcation diagram of model Eq. (1) without spatial forcing ($\gamma = 0$). We note that the bifurcation diagram is similar to the experimentally observed (cf. Fig. 2). When the bifurcation parameter is positive, the system exhibits coexistence between the $u = 0$ (nonoriented) unstable and the $u = u_+$ (reoriented, $0 = \mu + \beta u_+ + u_+^2 - u_+^4$) stable state. In this region of parameters, one expects to find FKPP fronts between uniform states. Figure 4(a) shows the typical front observed numerically.

In the coexistence region, when the spatial forcing is taking into account $\gamma \neq 0$, the zero state is persistent, since the

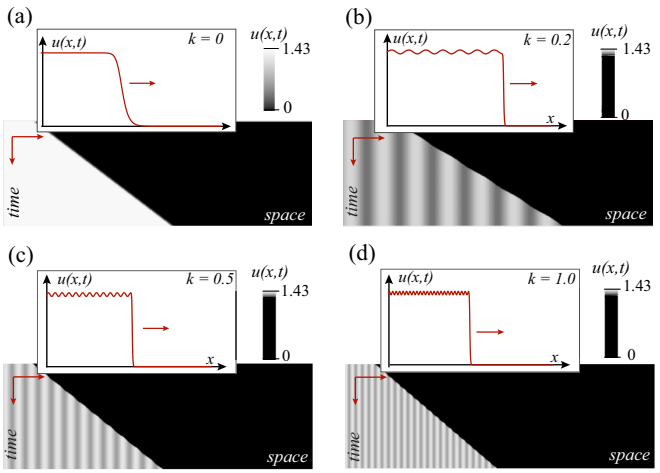

FIG. 4. Front propagation of model Eq. (1). Spatiotemporal diagram and front profile for $\mu = 1$, $\beta = 0.8$: (a) $\gamma = 0$, (b) $\gamma = 0.3$, and $k = 0.2$; (c) $\gamma = 0.3$ and $k = 0.5$; and (d) $\gamma = 0.3$ and $k = 1$.

forcing is proportional to the amplitude. However, the uniform stable state u_+ becomes a periodic one. Fronts propagation between these two states are observed when the unstable state is disturbed. Figure 4 shows the observed fronts into an unstable state in a forced medium when the forcing wave number is modified. Numerical simulations of fronts into an unstable state exhibit a fair agreement with the experimental observations. Numerically, we have characterized the average speed as a function of the bifurcation parameter, strength, and wave number of the forcing. Figures 5(a)–5(c) summarize the results. For small wave number k, the front speed decay as the forcing strength increases to a particular critical value, for which it begins to increase the front speed. For large wave numbers, always the front speed is increasing. Likewise, the front speed increases initially with the wave number, but for large values, it saturates and decays slowly.

When the characteristic experimental length of the width of the front is of the order of 10 μm (determined by the elastic constants and the rotation viscosity of the liquid crystal), and the characteristic length of the forcing is fractions of millimeters, then the proper physical limit of model Eq. (1) is a small wave number ($k \ll 1$). Hence, the experimental dynamical behavior of the front is consistent with the simplified model (1).

Front dynamics. To study the dynamics of fronts propagation into an unstable state in a forced medium, we consider the limit when the forcing is small ($\gamma \ll 1$). The unforced model Eq. (1) has front solutions of the form $u_0(x - vt - p_0)$, which does not have exact analytical solutions, but one can achieve excellent asymptotic approximations [5]. v is the front speed, and p_0 is the front position, corresponding to the spatial position where amplitude u has an equidistant value between the equilibria. The front is characterized by having the highest spatial variation around this point. To account for the forcing, we consider the following ansatz for the front solutions:

$$u(x,t) = u_0[x - p(t)] + w[x - p(t)], \tag{2}$$

where the front position is promoted to a temporal function and w is a small corrective function of the order of the perturbative term. Introducing the above ansatz in Eq. (1), linearizing in w, imposing the solubility condition, and after straightforward calculations, we get (see similar calculation with more detail in [22])

$$\dot{p} = v + \sqrt{K_1^2 + K_2^2}\cos(kp + \phi_0), \tag{3}$$

where $K_1 = \gamma\langle u_0(\xi)\sin(k\xi)|\psi\rangle/\langle\partial_\xi u_0|\psi\rangle$, $K_2 = \gamma\langle u_0\cos(k\xi)|\psi\rangle/\langle\partial_\xi u_0|\psi\rangle$, $\tan(\phi_0) = K_1/K_2$, $\xi \equiv x - vt - p$ is the coordinate in the mobile reference system, ψ is an auxiliary function that satisfies the linear equation $(v\partial_\xi - \mu - 2\beta u_0 - 3u_0^2 + 5u_0^4 - \partial_{\xi\xi})\psi = 0$, which is calculated numerically [see Fig. 5(d)], and $\langle f|g\rangle \equiv \int_{-L}^{L} f(\xi)g(\xi)d\xi$ is an inner product, where $2L$ is the system size. The previous coefficients are evaluated numerically, and we compare the front speed

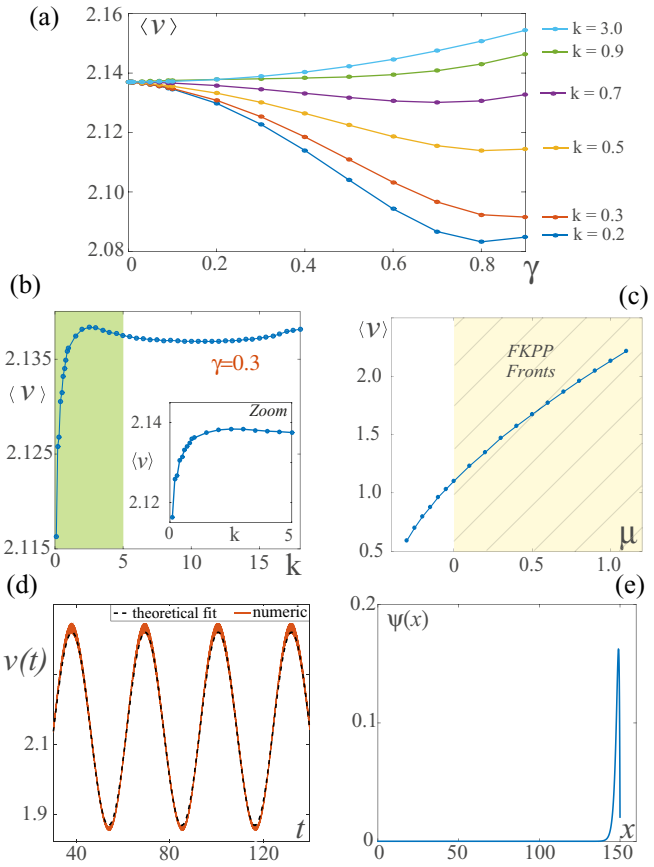

FIG. 5. Characterization of the front propagation speed of model Eq. (1). Average speed as a function of the strength (a) and wave number (b) of the forcing. The points are obtained from numerical simulations of model Eq. (1) with $\mu = 1.0$, $\beta = 0.8$, and the continuous curves emphasize the tendency of the front speed. (c) Average speed as a function of bifurcation parameter μ. The painted area accounts for the region of coexistence between a stable and unstable state. (d) Instant front speed as a function of time. The points are obtained from numerical simulations of model Eq. (1). The continuous line is obtained used formula (3). (e) $\psi(x)$ auxiliary function used to compute formula (3), obtained numerically by solving the linear equation $(v\partial_\xi - \mu - 2\beta u_0 - 3u_0^2 + 5u_0^4 - \partial_{\xi\xi})\psi = 0$.

formula (3) with the front speed obtained directly from Eq. (1) [see Fig. 5(c)]. We have quite a good agreement.

From Eq. (5) of the front position, one finds that the dynamic of the front is equal to an overdamped particle in a washboard potential. That is, the front Eq. (3) satisfies a ratchet motion equation [23]. Therefore, close to saddle-node instability, one expects the front to propagate slowly as a result of the ghost effect [24]. Namely, the particle alternates a drift force between a finite positive and a near to zero value. In this former regime, the particle moves slowly. Hence, this explains why the spatial forcing generates that the front spreads slowly in the presence of small forcing.

Conclusions. We show here how the propagation speed of a front into an unstable state can be modified using a spatial forcing. The front propagation exhibits a ratchet motion. The front's average speed decreases when the strength of the forcing increases. Hence, we present a simple strategy that can handle the nonlinear wave propagation using the spatial forcing.

Acknowledgments. C.C.P., M.G.C., and G.G-C. are thankful for the financial support of Millenium Institute for Research in Optics (MIRO). G.G-C. and K.A-B. acknowledge the financial support of CONICYT by Doctorado Nacional 2017-21171672 and 2014- 21140668, respectively.

[1] G. Nicolis and I. Prigogine, *Self-Organization in Nonequilibrium Systems* (Wiley, New York, 1977).
[2] H. Haken, *Synergetics, an Introduction: Nonequilibrium Phase Transitions and Self-Organization in Physics, Chemistry, and Biology* (Springer-Verlag, New York, 1983).
[3] H. Poincaré, L'Equilibre d'une masse fluide animée d'un mouvement de rotation, Acta Math. **7**, 259 (1885).
[4] L. M. Pismen, *Patterns and Interfaces in Dissipative Dynamics* (Springer, Berlin, 2006).
[5] J. D. Murray, *Mathematical Biology I and II* (Springer-Verlag, New York, 2001).
[6] M. Cross and H. Greenside, *Pattern Formation and Dynamics in Nonequilibrium Systems* (Cambridge University Press, New York, 2009).
[7] J. S. Langer, Instabilities and pattern formation in crystal growth, Rev. Mod. Phys. **52**, 1 (1980).
[8] M. Faraday, *Course of Six Lectures on the Chemical History of a Candle* (Griffin, Bohn & Co., London, 1861).
[9] R. A. Fisher, The wave of advance of advantageous genes, Ann. Eugenics **7**, 355 (1937).
[10] A. Kolmogorov, I. Petrovsky, and N. Piscounov, Study of the diffusion equation with growth of the quantity of matter and its application to a biology problem, Bull. Moscow Univ., Ser. Int A **1**, 1 (1937).
[11] P. Y. Front, Motion metastability and subcritical bifurcations in hydrodynamics, Physica D **23**, 3 (1986).
[12] W. Van Saarloos, Front propagation into unstable states, Phys. Rep. **386**, 29 (2003).
[13] D. G. Aronson and H. F. Weinberger, Multidimensional nonlinear diffusion arising in population dynamics, Adv. Math. **30**, 33 (1978).
[14] G. Ahlers and D. S. Cannell, Vortex-Front Propagation in Rotating Couette-Taylor Flow, Phys. Rev. Lett. **50**, 1583 (1983).
[15] J. Fineberg and V. Steinberg, Vortex-Front Propagation in Rayleigh-Bénard Convection, Phys. Rev. Lett. **58**, 1332 (1987).
[16] T. R. Powers and R. E. Goldstein, Pearling and Pinching: Propagation of Rayleigh Instabilities, Phys. Rev. Lett. **78**, 2555 (1997).
[17] J. Langer, *An Introduction to the Kinetics of First-Order Phase Transition*, Solids Far from Equilibrium (Cambridge University Press, Cambridge, 1992).
[18] M. G. Clerc, T. Nagaya, A. Petrossian, S. Residori, and C. S. Riera, First-order Fréedericksz transition and front propagation in a liquid crystal light valve with feedback, Eur. Phys. J. D **28**, 435 (2004).
[19] F. J. Elmer, J. P. Eckmann, and G. Hartsleben, Dual fronts propagating into an unstable state, Nonlinearity **7**, 1261 (1994).
[20] M. G. Clerc, S. Residori, and C. Riera, First-order Fréedericksz transition in the presence of a light driven feedback, Phys. Rev. E **63**, 060701 (2001).
[21] S. Residori, Patterns, fronts and structures in a liquid-crystal-light-valve with optical feedback, Phys. Rep. **416**, 201 (2005).
[22] K. Alfaro-Bittner, M. G. Clerc, M. A. Garcia-Nustes, and R. G. Rojas, π-kink propagation in the damped Frenkel-Kontorova model, Europhys. Lett. **119**, 40003 (2017).
[23] R. Feynman, *Lectures on Physics* (Addison-Wesley, Reading, MA, 1963), Chap. 46, Vol. I.
[24] S. H. Strogatz, *Nonlinear Dynamics and Chaos: With Applications to Physics, Biology, Chemistry, and Engineering* (CRC Press, Boca Raton, 2018).